ELSEVIER

Polymer 43 (2002) 5615–5621

polymer

www.elsevier.com/locate/polymer

Structural changes during isothermal crystallization of a poly(bisphenol A-*co*-decane ether) polymer

Yong Jiang[a,1], Qun Gu[a], Lin Li[a,*], De-Yan Shen[a], Xi-Gao Jin[a], Yu-Guo Lei[b], Chi-Ming Chan[b,*]

[a]*State Key Laboratory of Polymer Physics and Chemistry, Center for Molecular Science, Institute of Chemistry, Chinese Academy of Sciences, Beijing 100080, People's Republic of China*

[b]*Department of Chemical Engineering, Hong Kong University of Science and Technology, Clear Water Bay, Hong Kong, People's Republic of China*

Received 12 February 2002; received in revised form 31 May 2002; accepted 10 July 2002

Abstract

The isothermal crystallization behavior of a poly(bisphenol A-*co*-decane) (BA-C10) at 35 °C was studied in situ using polarized optical microscopy, atomic force microscopy (AFM) and Fourier transform infrared spectroscopic (FT-IR) measurements. Real-time FT-IR investigation revealed that an increase in regularity as well as intermolecular chain packing of certain functional groups of the BA-C10 main chains during crystallization. Our real-time AFM and FT-IR results provide an understanding of the relationship between the polymer morphology and the chain conformation during polymer crystallization. © 2002 Published by Elsevier Science Ltd.

Keywords: Isothermal crystallization; Fourier transform infrared spectroscopy; Atomic force microscopy

1. Introduction

Polymer crystallization has been extensively studied over the past several decades [1–7]. Chain folding in a single lamellar crystal of a semicrystalline polymer, which was first proposed by Keller [1] in 1957, is a common crystalline structure observed in many polymer systems. Many studies have been performed to investigate the detailed structure and formation mechanisms of polymer crystals using various methods, such as differential scanning calorimetry (DSC), wide-angle X-ray diffraction (WAXD), transmission electron microscopy (TEM), atomic force microscopy (AFM), nuclear magnetic resonance spectroscopy (NMR) and Fourier transform infrared spectroscopy (FT-IR). Among these methods, FT-IR spectroscopy has proved to be a powerful method for investigation of real-time conformational and structural changes during isothermal crystallization processes [8–17]. Vibrational modes that are quite sensitive to molecular symmetry can be used to detect different conformational changes during crystallization. The conformational change of various polymers such as syndiotactic polystyrene [8,10,11], poly(ethylene terephthalate) [12,13], polyimide [14], poly(propylene terephthalate) [15], syndiotactic and isotactic polypropylene [16,17] during the crystallization processes have also been studied by FT-IR spectroscopy.

It is well known that spherulites are common crystalline structures in semicrystalline polymers. The early studies performed with optical microscopy suggested that a spherulite consists of radiating fibrous crystallites [18,19]. Electron microscopic investigations revealed that a spherulite is composed of stacks of lamellae and amorphous regions between the lamellae [20,21]. Recent studies using tapping-mode AFM have made great advances in the understanding of lamellar growth and spherulitic formation because of the high resolution and the ability to image a dynamical process, in particular crystallization and melting in this technique [22–24]. Many AFM studies have been performed to investigate spherulitic structures [25–27], including the measurement of the overall growth rate of spherulites and the growth rate of lamellae [28,29].

Recently, Li et al. [27,28,30] synthesized a series of poly(bisphenol A-*co*-alkyl ether) (BA-Cn), which has a slow crystallization rate. The BA-Cn polymer's have been shown to be an ideal candidate for investigation of polymer crystallization at room temperature with AFM. With the advantages of BA-Cn and AFM, the detailed construction process of the spherulites has been described. Furthermore, the BA-Cn polymer's have various functional groups such

* Corresponding authors. Tel.: +86-10-6257-1067; fax: +86-10-6256-9373.

E-mail address: lilin@pplas.icas.ac.cn (L. Li).

[1] Present address: Graduate School of the Chinese Academy of Sciences.

0032-3861/02/$ - see front matter © 2002 Published by Elsevier Science Ltd.
PII: S0032-3861(02)00441-X

as phenyl ring, carboxyl group and the flexible alkyl segments. The characteristic peaks of these functional groups in the infrared spectra enable us to analyze the changes during the crystallization in real-time. In this work, the formation of spherulites of BA-C10 was investigated using POM and AFM. FT-IR spectroscopy was utilized to study the changes in the conformation and crystallinity of the BA-C10 during crystallization.

2. Experimental section

A sample of BA-C10 was synthesized by condensation polymerization of bisphenol A and 1,10-dibromodecane [30]. The glass transition temperature, melting point, number-average molecular weight, and polydispersity index were measured to be 10.5 °C, 83.3 °C, 11,500 g/mol, and 2.6, respectively.

The growth process and the morphology of the spherulites were observed at 35 ± 0.5 °C using a polarized optical microscope (OLYMPUS BH-2) equipped with a Mettler hot stage. Tapping-mode AFM images were obtained at 35 ± 0.5 °C using a NanoScope III *Multi-Mode*™ AFM (Digital Instruments) equipped with a hot stage. Silicon cantilever tips with a resonance frequency of ~300 kHz and a spring constant of ~40 N m^{-1} were used. The scan rate ranged from 0.5 to 1.5 Hz/s. The sample line was 512 and the target amplitude was 2 V. Height and phase images were recorded simultaneously during scanning. In this paper, we show only the phase images that best reveal the morphological features. Thin films were prepared by spin coating 30 mg ml^{-1} polymer–chloroform solutions at 3000 rpm onto silicon wafer surfaces (10 mm × 10 mm). The thickness of the amorphous BA-C10 film was estimated to be about 300 nm.

In situ FT-IR measurements were made using a Bruker Equinox-55 FT-IR spectrometer equipped with a Specac variable temperature cell at 35 °C. To prevent condensation of moisture to the sample at low temperatures, the sample cell was kept under vacuum during the measurement. In order to measure the instantaneous spectral changes, a liquid nitrogen cooled MCT detector with the resolution of 4 cm^{-1} was used. A total of 32 scans were made and the scanning was repeated every 180 s. A small amount of 4 wt% BA-C10 chloroform solution was cast on a KBr plate. After the solvent was evaporated, the plate was heated to 100 °C for 10 min to melt the polymer and finally it was quenched to 35 °C. The FT-IR spectra were obtained as the polymer crystallized.

3. Results and discussion

3.1. Morphological changes

Fig. 1 shows a series of polarized optical micrographs showing the growth process of a spherulite. The sheaflike structures as shown in Fig. 1a and b can be clearly observed during the early growing stages of the spherulite. Gradually, the lamellar sheaves diverge and fan outward to form a skeleton of the spherulite. After repeated splaying, the lamellae form a spherical shape characteristic of a spherulite, as shown in Fig. 1c and d. Because of the large steric hindrance of the bisphenol A group in the backbone of BA-C10, the rate of the crystallization is slow and the structure of the spherulite is not perfect. As indicated by the arrows in Fig. 1e, there are two defects generated during the growth of the spherulite. New fan-shaped lamellae grow from these two defects. In order to get a better understanding of the formation of the spherulite, the surface morphological changes during the crystallization of the BA-C10 polymer thin film were also studied using an AFM equipped with a heating stage.

Fig. 2 shows a series of the AFM phase images of the BA-C10 thin film crystallized at 35 °C at different time intervals. The growth of edge-on lamellae and the formation of the spherulites can be clearly observed. The lamellae with an edge-on orientation grow preferentially on these polymer thin films, consistent with our earlier observations on similar polymer films [27,28]. The AFM phase shows more detailed information about the crystalline structure compared with the POM images. As shown in Fig. 2a and b, a single lamella breeds more lamellae that develop into an embryo of a spherulite. The primary lamella can grow at both ends and it breeds more lamellae through secondary nucleation. The lamellae developed from the secondary nucleation splay apart from each other and breed more lamellae. As a result of this continuous growing, splaying and breeding of secondary lamellae, the initial lamella gradually evolves into a lamellar sheaf, as shown in Fig. 2c and d. Fig. 2e and h shows the process of a lamellar sheaf developing into a spherulite skeleton upon further growth of the lamellae.

The growth rate is an important issue in any kinetic study. Many studies have been performed to measure the growth rate of spherulites using optical microscopy and using recently AFM [28,31]. It has been predicted by theoretical models and observed experimentally that the overall spherulitic growth rate is constant. It should be noted that these observations were made from the middle stage of the growth of spherulites when a large number of lamellae were growing at the same time. Theoretical models have also predicted the growth rate of a single lamella to be constant. However, AFM investigations produced contradictory results. They showed that some lamellae initially grew forward faster than the overall growth rate of spherulites, and the growth rate was not constant and different for individual lamella. Even in the same lamellae, the growth rate varied at different locations. Recently, we found that a stable embryo grows into a founding lamella and there is only one founding lamella in each spherulite. The growth rate of the founding lamella was found to be

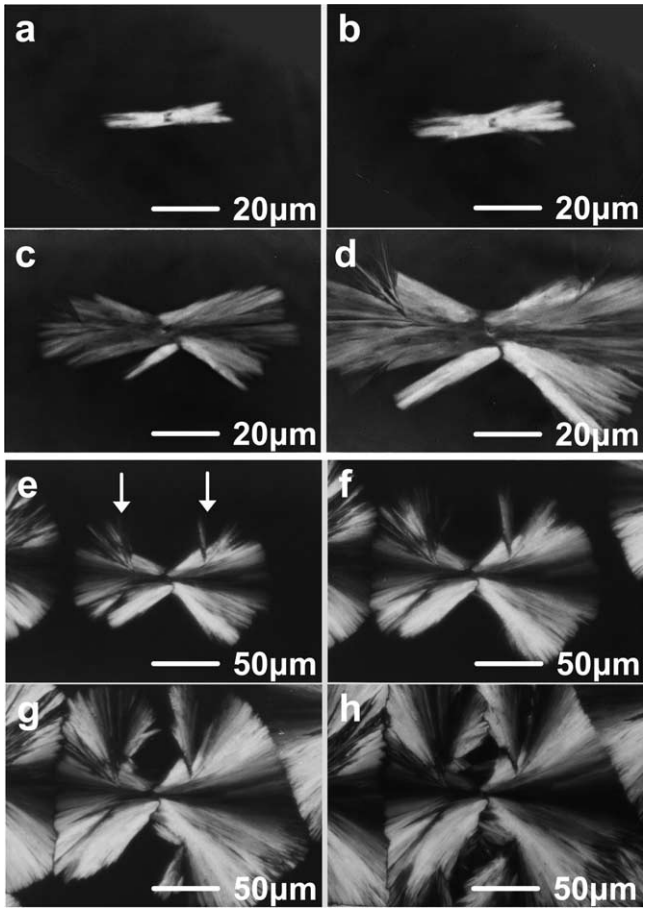

Fig. 1. Optical micrographs of the BA-C10 isothermal crystallized from melt at 35 °C. The photos were taken at 250, 270, 290, 320, 350, 370, 400, and 420 min after the film was prepared.

relatively constant at the initial stage of the formation of spherulites [32].

From our observations, it is clear that when the amorphous film is allowed to crystallize at 35 °C, which is above its glass transition temperature of 10.5 °C, the polymer chains can relax and fold into the lattice of lamellae and form spherulites. The above AFM observation can provide very valuable information about the development of the random polymer coils into spherulites. The largest diameter of the spherulite shown in Fig. 2 was measured as a function of time at 35 °C. The results are shown in Fig. 3. The size of the spherulite increases linearly with time, suggesting that the overall growth rate of the spherulites is constant. It is important to point out that with higher resolution AFM images, the earlier period of the crystallization can be observed. The first lamella appeared about 150 min after the film was prepared. Any conformational changes during this long induction period could not be observed by AFM. Therefore, in situ FT-IR measurements were used to study the conformational changes during the crystallization of the BA-C10 polymer.

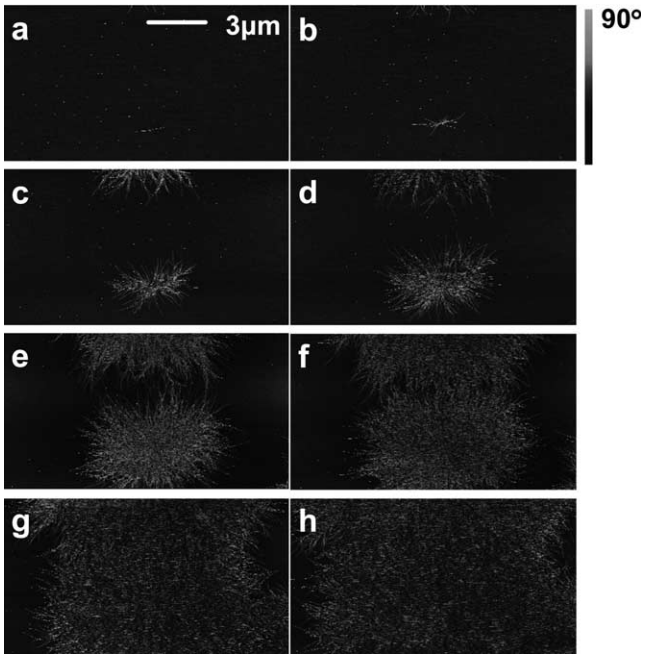

Fig. 2. AFM phase images of a BA-C10 thin film, taken during isothermal crystallization at 35 °C on an AFM heating stage. (a) Taken at 190 min after the film was prepared; (b–h) taken at a 32 min interval after (a).

3.2. Conformational changes

The IR spectra of amorphous and semicrystalline samples of the BA-C10 polymer, which are shown in Fig. 4, exhibit distinct differences. Table 1 summarizes the results obtained from the analysis of the FT-IR spectra and the assignment of each band.

Fig. 5 shows the IR spectra of the polymer as a function of time. As crystallization progressed at 35 °C, the intensities of some bands changed greatly and the others

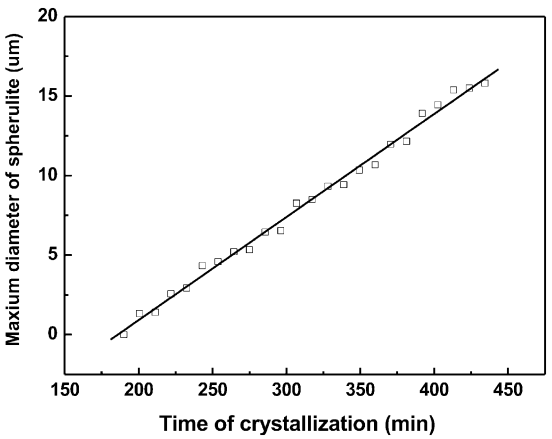

Fig. 3. The largest diameter of the spherulite determined by AFM as a function of crystallization time.

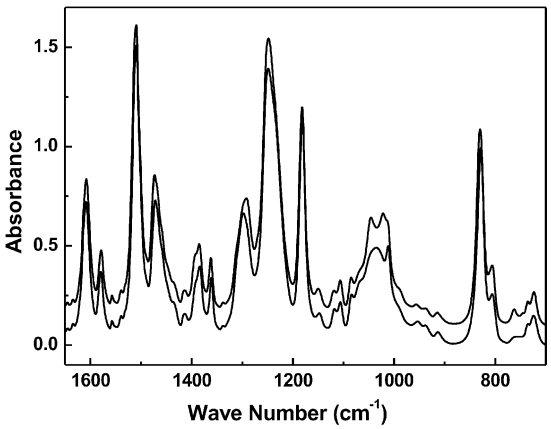

Fig. 4. FT-IR spectra of crystalline (upper) and amorphous (lower) BA-C10 samples. The crystalline sample was isothermally crystallized at 35 °C for 843 min.

showed a shift in the frequency. The bands at 1650–1450 cm^{-1}, which were assigned to the out-of-plane bending vibration of benzene rings, only showed slight changes, as shown in Fig. 5a. The band at 1292 cm^{-1}, assigned to the C–O stretch vibration of the benzene groups, shifted to higher wave numbers during crystallization. The shifting of this band to high wave numbers was probably caused by the appearance of a new peak at a high wave number that corresponds to the development of the crystalline phase. The convolution of the old and new peaks produced the observed shifting. Fig. 5b also shows that the intensity of peaks at 1248 and 1182 cm^{-1} increase and decrease, respectively. Among all the peaks, the peaks at 1035 and 1011 cm^{-1} corresponding to the C–O stretch vibration of the alkane groups showed the most distinct changes as crystallization progressed. This result suggests that the movement of the most flexible group, C–O, of the rigid segment of the repeat unit was severely restricted as the macromolecules packed into the lattices of polymer crystals. The peak at 830 cm^{-1}, which is the diagnostic vibration of the 1,4-substitute benzene ring, shows a slight shift to a higher wave number during crystallization. In the region between 700 and 800 cm^{-1}, the intensity of the peaks at 763, 747, 736,

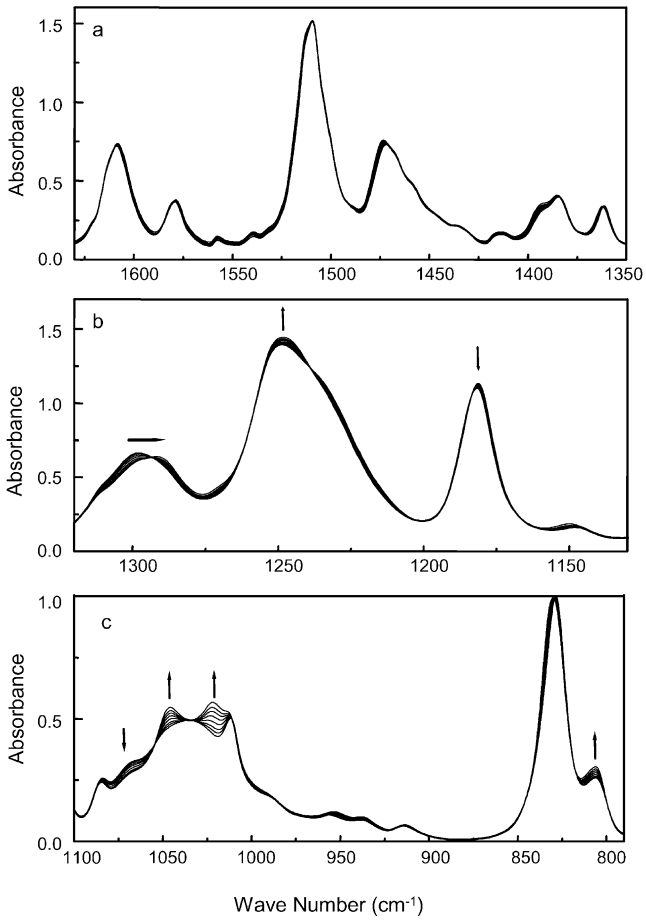

Fig. 5. Infrared spectra of the BA-C10 sample crystallized at 35 °C from the amorphous state. (a) 1650–1350 cm^{-1}; (b) 1330–1130 cm^{-1}; (c) 1100–780 cm^{-1}. The arrows show the change of the peaks with crystallization time.

and 723 cm^{-1}, which were assigned to the CH_2 rocking vibration of the alkane, increased during the crystallization (Fig. 6). Furthermore, the typical changes of the rocking bands indicate the regular packing of the folded chain due to the intermolecular interaction. The changes in the intensity of these peaks are important and valuable for the analysis of the isothermal crystallization behavior of the BA-C10 polymer.

Table 1
Infrared spectral changes upon crystallization of the BA-C10 polymer

Amorphous (cm^{-1})	Crystalline (cm^{-1})	Influence of crystallization (cm^{-1})		Probable assignment
1471.9	1473.3	← 1.4	↑	ν(C=C of phenyl ring)
1297.9	1291.8	→ 6.1	↓	ν(benzene C–O)
1035.1	1045.7	← 10.6	↑	ν(alkane C–O)
1011.7	1021.8	← 10.1	↑	ν(alkane C–O)
828.4	830.1	← 1.6	↓	Out of plane δ(benzene)
–	762.8	New peak	↑	$r(CH_2)$

→ and ←: shift to lower and higher wave number. ↑ and ↓: peak increase and decrease during crystallization. ν: stretch; δ: bending; r: rocking.

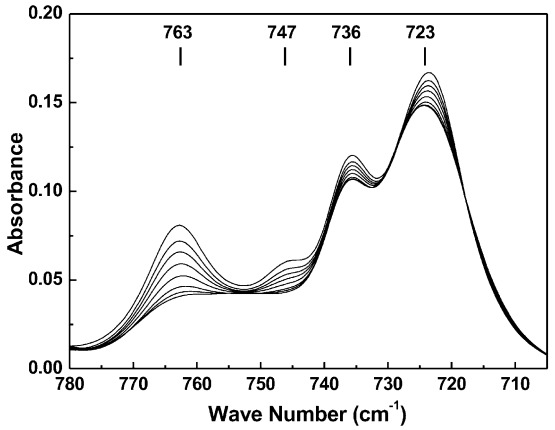

Fig. 6. In situ FT-IR measurements for the sample isothermally crystallized at 35 °C. The spectra displaced from the bottom to the top are measured at 61, 181, 242, 302, 362, 422, 482, and 843 min after the film was prepared.

It is also worth noting that the peaks between 700 and 800 cm^{-1} did not shift during the crystallization and all these peaks are separated from each other. Consequently, they can be used to analyze the isothermal crystallization behavior. In order to relate the change in the intensity of these peaks to the crystallization kinetics, a series of difference spectra were obtained by subtraction of the amorphous state spectrum from the semicrystalline state spectrum. In order to take into the account the thickness changes during isothermal crystallization, the peak at 2845 cm^{-1} was chosen as the internal reference. After the adjustment of the sample thickness, the difference spectra obtained by this method are shown in Fig. 7. It can be seen clearly that the intensity of the four peaks increased as the crystallization proceeded.

The peak heights of the four peaks at 763, 747, 736, and 723 cm^{-1} were measured using the OPUS software. The peak height which is related to the crystallinity of the sample increased with the crystallization time, as shown in

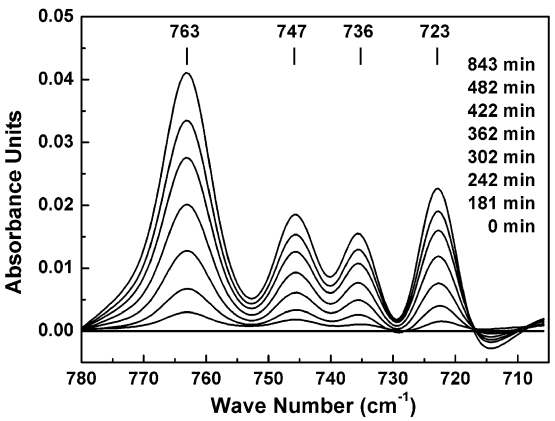

Fig. 7. Difference spectra for the sample isothermal crystallized at 35 °C, as shown in Fig. 6. The spectra displaced from the bottom to the top are measured at 61, 181, 242, 302, 362, 422, 482, and 843 min after the film was prepared as shown.

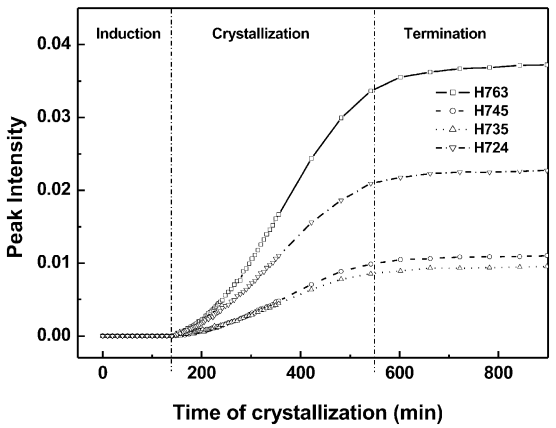

Fig. 8. The intensity of the peaks at 763, 747, 736, and 723 cm^{-1} as a function of time during isothermal crystallization at 35 °C.

Fig. 8. The crystallization process can be divided into the following stages: induction period, crystallization period and termination period. In the induction period, the peak heights of the four peaks stay rather constant. In the crystallization period, the intensities of these crystalline peaks increase slowly at the beginning and then increase linearly with time. In the termination period when the spherulites impinge upon each other, there is almost no change in crystallinity.

Avrami's equation states that

$$\frac{A_t - A_\infty}{A_0 - A_\infty} = \exp(-kt^n) \tag{1}$$

where A_t is the peak intensity at the crystallization time t; A_∞ and A_0 are, respectively, the initial and final intensities of the peak during isothermal crystallization; k is the overall kinetic constant of crystallization; t is the crystallization time step measured after the thin film was prepared; and n is the Avrami exponent, which is related to the type of nucleation and to the geometry of the growing crystals. Eq. (1) can also be expressed in the following form:

$$\ln\left[-\ln\left(\frac{A_t - A_\infty}{A_0 - A_\infty}\right)\right] = \ln k + n \ln t \tag{2}$$

Plotting the first term versus $\ln t$, both k and n can be obtained from the slope and the intercept at $\ln t = 0$, respectively. The half time for the crystallization, $t_{1/2}$, can also be calculated from k and n, with the following equation:

$$t_{1/2} = \left(\frac{\ln 2}{k}\right)^{1/n} \tag{3}$$

The results are shown in Table 2. The Avrami index, n, is 2, which can be attributed to heterogeneous nucleation taking place inside the quasi two-dimensional spherulite. The average half time of crystallization, $t_{1/2}$, is 221 min, which is consistent with the results of POM and AFM.

Table 2
Avrami parameters derived from the IR spectroscopic data

Peak region (cm^{-1})	Site of the peak on crystallization				
	763	746	736	723	Average
Rate constant, k ($\times 10^5$)	0.98	0.97	1.0	1.4	1.1
Avrami index, n	2.07	2.06	2.06	2.02	2.05
Half time, $t_{1/2}$ (min)	222	226	221	214	221

The FT-IR results indicate that the intensity and location of the IR peaks change during crystallization. In particular, there was a new peak emerging at 763 cm^{-1} as crystallization proceeded. The folding of the random polymer chains into the crystalline lattice involves the arrangement of various functional groups. The obvious changes in the IR spectra are the ν(C=C of phenyl ring), ν(benzene C–O), ν(alkane C–O), ν(alkane C–O), out of plane δ(benzene), and $\gamma(CH_2)$. Among them, the most flexible ether group C–O shows the greatest change. In the amorphous state, the flexible groups are mobile. However, in the crystalline state, the mobility of these flexible groups is highly restricted. Hence, the greatest change before and after the crystallization is observed in the most flexible group C–O. It took quite a long induction period before the peaks at 763, 747, 736, and 723 cm^{-1} appeared, indicating that the adjustment of the configurations and positions of the polymer chains to fit into crystals is a time-consuming process.

In the end, there is an important fact that must be clarified here. For the spectroscopic measurements, the results are the statistical average values of the whole areas measured. But for AFM, smaller areas can be observed, so the growth rate of a spherulite measured is an individual result.

Each spherulite was formed at a different time. The FT-IR measurements revealed the average changes of the characteristic bands of many spherulites during the BA-C10 crystallization. However, the observation on the formation of the spherulites using AFM showed the development of an individual spherulite. The induction periods for the primary nucleation of individual spherulites are significantly different as suggested by real-time AFM observations. Therefore, it is reasonable to observe the difference in the induction period as measured by FT-IR and AFM.

4. Conclusions

Unique infrared spectral peaks of the BA-C10 polymer appearing upon crystallization were identified. The results of isothermal crystallization by infrared spectroscopy with the results of POM and AFM were consistent. The crystallization process was found to involve intramolecular movements and intermolecular chain packing. Intermolecular movements about the flexible alkane chain and the ether group led to a state of increased coplanarity. Increased chain packing was reflected in the intermolecular interactions of the alkane groups. Crystallization kinetics parameters were determined using the peak intensities as a function of the crystallization time.

Acknowledgments

We are grateful for the support of National Science Foundation of China (Grant No. 20044005, 20174049 and 20131160730) and the Hong Kong Government Research Grants Council under Grant No. N_HKUST 618/01.

References

[1] Keller A. Phil Mag 1957;2:21.
[2] Hoffman JD, Miller RL. Polymer 1997;38:3151.
[3] Strobl G. Eur Phys J E 2000;3:165.
[4] Heck B, Hugel T, Iijima M, Strobl G. Polymer 2000;41:8839.
[5] Bassett DC. Principles of polymer morphology. Cambridge: Cambridge University Press; 1981.
[6] Lotz B. Eur Phys J E 2000;3:185.
[7] Geil PH. Polymer 2000;41:8983.
[8] Matsuba G, Kaji K, Nishida K, Kanaya T, Imai M. Macromolecules 1999;32:8932.
[9] Zhang D, Ward RS, Shen YR, Somorjai GA. J Phys Chem B 1997; 101:9060.
[10] Tashiro K, Ueno Y, Yoshioka A, Kobayashi M. Macromolecules 2001;34:310.
[11] Wu HD, Tseng CR, Chang FC. Macromolecules 2001;34:2992.
[12] Radhakrishnan J, Kaito A. Polymer 2001;42:3859.
[13] Jang J, Oh JH, Moon SI. Macromolecules 2000;33:1864.
[14] Ishida H, Huang MT. J Polym Sci, Part B: Polym Phys 1994;32: 2271.
[15] Bulkin BJ, Lewin M, Kim J. Macromolecules 1987;20:830.
[16] Nakaoki T, Yamanaka T, Ohira Y, Horii F. Macromolecules 2000;33: 2718.
[17] Zhu XY, Yan DY, Yao HX, Zhu P. Macromol Rapid Commun 2000; 21:354.
[18] Keller A. J Polym Sci 1955;17:291.
[19] Keith HD, Padden FJ. J Polym Sci 1959;39:101.
[20] Keller A, Sawada S. Makromol Chem 1964;74:190.
[21] Bassett DC, Hodge AM, Olley RH. Proc R Soc Lond 1981;A377:25. see also pages 39 and 61.
[22] Magonov SN, Elings V, Whangbo MH. Surf Sci 1997;375:385.
[23] Bar G, Thomann Y, Brandsch R, Cantow HJ, Whangbo MH. Langmuir 1997;13:3807.
[24] Bar G, Delineaua L, Brandscha R, Brucha M, Whangbob MH. Appl Phys Lett 1999;75:4198.
[25] Haeringen DTV, Varga J, Vancso GJ, Ehrenstein GW. J Polym Sci, Part B: Polym Phys 2000;38:672.
[26] Godovsky YK, Magonov SN. Langmuir 2000;16:3549.
[27] Li L, Chan CM, Li JX, Ng KM, Yeung KL, Weng LT. Macromolecules 1999;32:8240.
[28] Li L, Chan CM, Yeung KL, Li JX, Ng KM, Lei YG. Macromolecules 2001;34:316.

[29] Basire C, Ivanov DA. Phys Rev Lett 2000;85:5587.
[30] Li L, Chan CM, Ng KM, Lei YG, Weng LT. Polymer 2001;42:6841.
[31] Hobbs JK, McMaster TJ, Miles MJ, Barham PJ. Polymer 1998;39: 2437.
[32] Lei YG, Chan CM, Li JX, Ng KM, Jiang Y, Li L. The birth of an embryo and development of the founding lamella of spherulites as observed by atomic force microscopy. Macromolecules (in press).